Supplementary Movie 1). Furthermore, these GFP-marked structures were co-localized with *in vivo* biotin-labeled membrane (Figure 7D), indicating that EndA1-BAR296-induced fibrous structure seems to be a membrane invagination originated from the plasma membrane. These structures were found in other cells we tested (Figure 7C). In clear contrast, ΔApp, ΔNT and a4 were incapable of inducing membrane deformation in cells, indicating the importance of helix 0, the rigid crescent shape, and the appendage of BAR domain for membrane deformation *in vivo*.

Discussion

The endophilin-A1 BAR domain dimer consists of three sub-modules: the crescent-shaped main body, the helix 0 and the unique appendage. We tried to understand the functional roles for these sub-modules in the membrane curvature formation. In this study by determining the structure of endopholin-A1 BAR domain and developing mutants that were critical for the sub-module structure, we have explored the roles of sub-modules.

Here, we show that the structural rigidity of the crescent-shaped main body is critical for membrane tubulation. The BAR dimer is sufficiently rigid to overcome the bending resistance of the membrane and to be scaffolds for the tubulation (McMahon and Gallop, 2005; Zimmerberg and Kozlov, 2006). The insertion of one helical-pitch into the helix II at distal to the kink brings flexibility to the dimer (a4 mutant). The relative position of the three helices in the

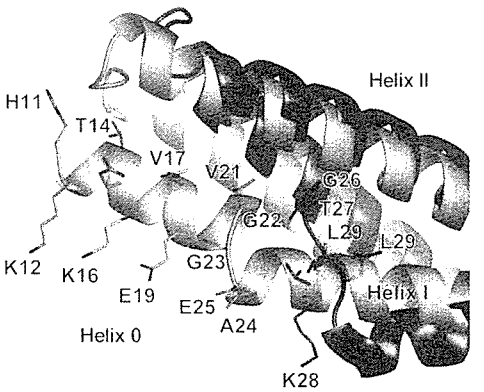

Figure 6 Close-up of helix 0 in an a4 mutant monomer (orange). The same superimposition as in Figure 5C but viewed from the side and displays the helix 0. The helix 0 is disordered in the wild-type structure (blue). The side chains of N-terminal residues are shown (H11KATQKVSEKVGGAEGTKL29 in the a4 and G26TKL in the wild type). The amphipathic helix 0 is stabilized by hydrophobic interactions with the helix II and III and also by hydrogen bonds with a symmetrical molecule.

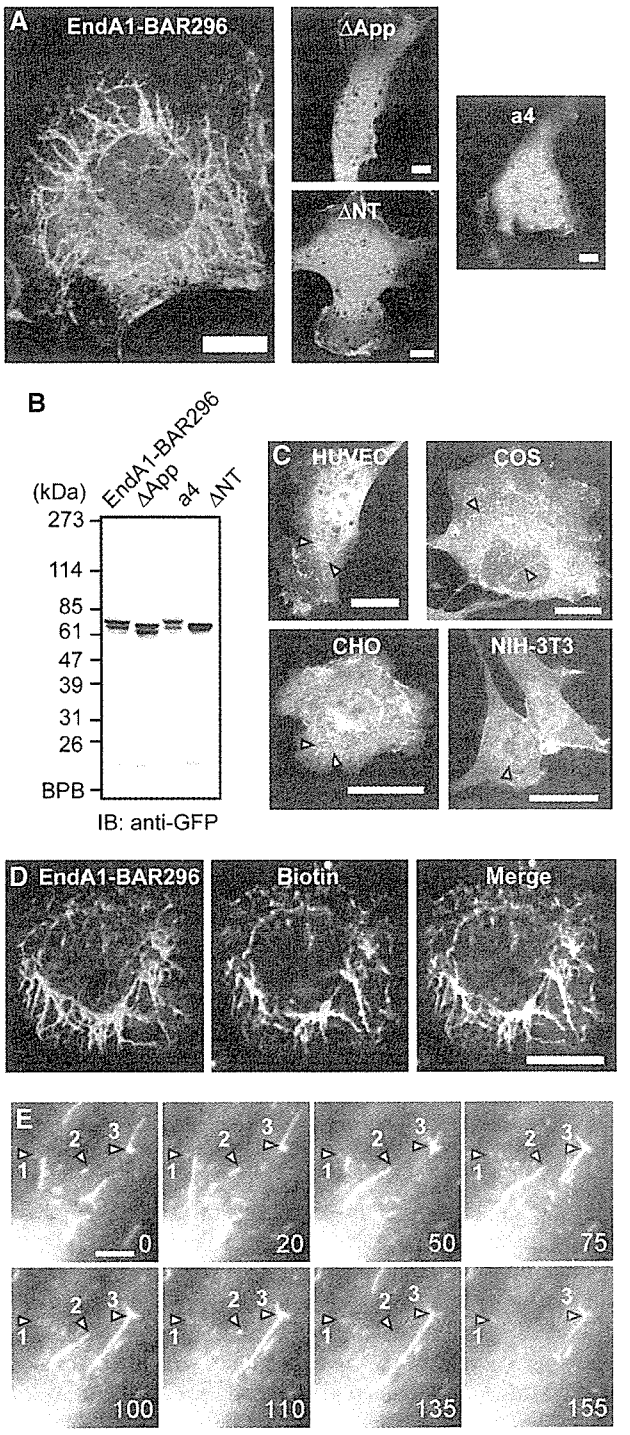

Figure 7 Endophilin A1 BAR domain induces membrane tubulation *in vivo*. (**A**) HUVECs were transfected with plasmids expressing C-teminally EGFP-tagged EndA1-BAR296 (amino acid 1–296 of endophilin-A1), ΔApp, a4, and ΔNT. Cells were GFP-imaged on an epifluorescnce microscope (Olympus IX-71). Fibrous structures were observed exclusively in EndA1-BAR296-expressing cells. Scale, 10 μm. (**B**) Protein expression of the EndA1-BAR296 and the mutants tagged with EGFP in transfected 293T cells were examined by immunoblotted with anti-GFP antibody. (**C**) Cells indicated were similarly transfected to (A). Arrowheads indicate the fibrous structures. Scale, 20 μm. (**D**) Live HUVECs expressing EGFP-tagged EndA1-BAR296 were biotinylated with sulfo-NHS-biotin for 10 min and chased for further 10 min. Covalently bound biotin was visualized using Alexa633-streptavidine. Fluorescnece images for EGFP (left), Alexa633 (center), and merge (right) are shown. Scale, 10 μm. (**E**) A time lapse images of HUVECs expressing EGFP-tagged EndA1-BAR296 were obtained at the time point (seconds) after the observation (Supplementary Movie 1). EGFP-marked structure grows from the cell periphery towards the center of the cell. Notably, both extension and retraction of GFP-marked structure is observed (numbered arrow heads indicate each extending/retracting structure). Scale, 5 μm.

mutant arm was not changed in a4 mutant irrespective of the bend levels (Supplementary Figure 8). The mutant arm behaves as a rigid body and its structure changes only in the vicinity of the helix kinks when it swings. Therefore, it is unlikely that the flexibility of the mutant dimer can be a result of weakened inter-helix interactions in the arm. Moreover, we could not find any specific structural features in the kink region that might explain the flexible hinge in the swinging-arm mutant as well as the rigid bend in the wild-type BAR dimers of endophilin, amphiphysin, and arfaptin.

In this study, for the first time we could determine the structure of the N-terminal amphipathic helix (helix 0) using a swinging-arm mutant. Our mutant and previous mutation analyses indicated that the N-terminal helical sequence of endophilin-A1 is indispensable for liposome binding (Farsad *et al*, 2001), whereas that of amphiphysin is important but not essential for liposome binding and tubulation (Peter *et al*, 2004). The BAR domain of endophilin-A1 is an acidic polypeptide and the cluster of positive charge at the distal end of the arm is not prominent (Figure 1A). This property can explain the critical role for the helix 0 of the EndA1-BAR in liposome binding by providing additional basic residues. The helix 0 structure suggests that K12, K16 and possibly K8 are in a suitable position for cooperation with the positive charge cluster at the distal end. The amphipathic nature of the helix 0 implies that it can also insert into the membrane and facilitate the membrane curvature formation (Peter *et al*, 2004; Gallop and McMahon, 2005; McMahon and Gallop, 2005). Loss of the membrane-deforming activities of the A66D mutant (Figure 2) and the a4ΔApp mutant (Figure 5D) accounts for the additional mechanism for membrane deformation in addition to the membrane insertion of the helix 0.

The N-BAR of endophilins has one additional step to tubulate membrane. Here, we show that the hydrophobic ridge of the endophilin-specific appendage is inserted into the contacting membrane surface. Our data suggested that the entire ridge of the wild-type BAR domain, about 8 Å in height, is embedded in the layer of lipid head-groups of the contacting membrane leaflet. The embedding of the ridge into the membrane is consistent with the local spontaneous curvature mechanism that is reported very recently (Zimmerberg and Kozlov, 2006). As a protruding structure found in epsin1 induces liposome tubulation by being inserted to one leaflet of the lipid bilayer (Ford *et al*, 2002), the penetration of the hydrophobic ridge can drive the positive curvature by causing asymmetrical expansion of the surface area between two leaflets as shown in Figure 8 (Farsad and De Camilli, 2003).

We further explored the importance of the ridge, rigid crescent shape, and helix 0 in cells. We for the first time showed that N-BAR domain induced membrane invaginations originated from plasma membrane, although other BAR-containing molecules have been reported to induce similar invaginations (Itoh *et al*, 2005). Neither mutant that lacked either the ridge or the helix 0 nor flexible mutant formed the tubular invaginations in cells, indicating the significance of these sub-module structure in cells as suggest by *in vitro* studies. We constructed a series of endorphin-A1-EGFP expression plasmids to delineate the domain for the membrane invagination. Full-length endophilin-expressing cells did not show any tubular formation. Because endophilin consists of BAR domain and an SH domain, SH3-binding molecule such as dynamin may inhibit the extension of membrane invagination. This possibility has been suggested in the membrane invagination found in FBP17 and amphiphysin (Kamioka *et al*, 2004; Itoh *et al*, 2005).

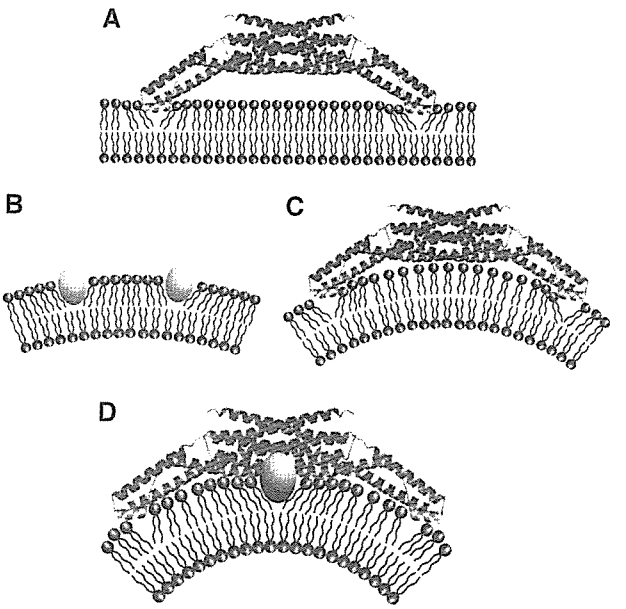

Figure 8 Two potential mechanisms for driving membrane curvature by endophilin-A1. (**A**) Kissing adhesion of an N-BAR domain on planar lipid bilayer. The helix 0 is essential for the membrane binding. Membrane insertion of the helix 0 is supposed. (**B**) Insertion of hydrophobic portions of macromolocules into one leaflet can create bilayer surface discrepancy that causes membrane curvature. (**C**) The simple N-BAR domain, such as amphiphysin and ΔApp, induces membrane curvature by impressing the concave surface onto the membrane. The rigidity of the molecule is required for this mechanism. (**D**) To drive membrane curvature, the endophilin N-BAR domain uses both the rigid crescent shape-mediated deformation and the insertion of hydrophobic ridge on the concave surface in addition to kissing adhesion of N-BAR to membrane surface.

Collectively, EndA1-BAR uses two newly identified mechanisms to drive positive membrane curvature in addition to the essential binding capacity of helix 0 to the membrane: one by the scaffold mechanism common to the BAR domains and the other by the local spontaneous curvature mechanism caused by the membrane insertion of the ridge (Figure 8D). The ridge, which occupies the bottom of the concave lipid-binding surface, may not work until the main body of the BAR dimer localizes itself to a curved membrane. The ridge then inserts into the bilayer roughly perpendicular to the main body, and thus both deformations will occur in the same direction.

Materials and methods

Protein expression and purification by CRECLE

cDNAs encoding BAR domains (amphiphysin1, 1–239; endophilin-A1, 1–247; endophilin-B1, 1–246 in amino-acid residues) were amplified by PCR from a human brain cDNA library. Recombinant proteins were expressed in *Escherichia coli* as GST-fusions using the pGEX6p3 vector, purified by glutathione-Sepharose, cleaved from the GST-tag using Prescission protease (Amersham Biosciences), and further purified by ion-exchange chromatography (Yamagishi *et al*, 2004). The final polypeptide contained an artificial linker

sequence of GPLGS at the N-terminus. EndA1-BAR proteins except for F202W and a4 mutants were purified by crystallization during Prescission protease cleavage. The method, crystallization by regulated cleavage of large hydrophilic tag (CRECLE), was as follows. Purified GST fusions were concentrated to 20–30 mg/ml in an elution buffer (20 mM glutathione, 100 mM Tris-HCl, pH 8.0, 10 mM DTT, 1 mM EDTA, 1 mM EGTA) and then cleaved by a low concentration of prescission protease (1 U/mg protein or less) at 4°C. Slow increase in the tag-free protein concentration might be suitable for crystallization and more than a half of EndA1-BAR protein could be recovered as 20–100 μm microcrystals. They were washed with a low-salt buffer (20 mM HEPES, pH 7.4, 2 mM DTT, 0.2 mM EDTA, 0.2 mM EDTA) and resolved into a high-salt buffer (350 mM NaCl in the low-salt buffer) and used for further analyses.

Protein crystallization

Seleno-methionine (S-Met) derivatives of the EndA1-BAR domain and its appendage-less mutant (ΔApp) were produced in B834(DE3)pLysS cells using Overnight Express Autoinduction System 2 (Novagen). To make X-ray grade crystals in a cryo-ready condition, modified high salt buffer (50 mM HEPES, pH 7.4, 300 mM NaCl, 100 mM KI, 28% ethylene glycol, 5% glycerol, 25 mM DTT) was used. Crystals of 1 mm size were formed by dialysis against 50 mM CHES, pH 9.5, 260 mM NaCl, 28% ethylene glycol, 5% glycerol, 25 mM DTT, 0.4% benzamidine · HCl at 4°C and were flush frozen at 100 K. Crystals could also be grown by vapor diffusion from a similar protein solution using distilled water as the bath solution. The crystals were equilibrated in 50 mM HEPES, pH 7.4, 150 mM NaCl, 25 mM DTT, 0.4% benzamidine · HCl, 5% PEG 8000 and the saturated amount of xylitol as a cryoprotectant. Some of the crystals were soaked with 0.5 mM oleoyl-L-α-lysophosphatidic acid (Sigma) or malonyl-CoA (Sigma) for 4 days with daily change for the substrates. The a4 mutant crystals were grown by sitting-drop vapour diffusion using a bath solution containing 100 mM HEPES, pH 7.2, 200 mM calcium acetate, 10 mM DTT and 20% (w/v) PEG3350 at 20°C and then flush frozen after brief immersion in the same solution containing 16% DMSO. The wild type and the ΔApp mutant crystals belong to the same space group $I4_1$ and contain one monomer molecule in the asymmetric unit (Supplemental Figure 1). The a4 crystal belongs to $P2_1$ and contains two dimers in the asymmetric unit.

Structural determination

The EndA1-BAR structure was determined using the multiple anomalous dispersion (MAD) method. Multiple-wavelength X-ray diffraction data sets were collected from a single Se-Met crystal (crystal I) at SPring-8 beamline BL44B2 (Supplementary Table I). Single wavelength data sets of another crystal (crystal II) and of a ΔApp crystal used for the refinement were collected at BL45PX. The data set for the a4 mutant was collected at BL38B1. All diffraction data sets were collected at 90 K and were processed using HKL2000 suite (Otwinowski and Minor, 1997). The seven positions out of 10 expected selenium atoms were identified by SOLVE (Terwilliger and Berendzen, 1999). The initial phases calculated by SOLVE with a figure of merit of 0.59 at 3.2 Å resolution were further improved by RESOLVE (Terwilliger, 1999). The density modified MAD map (Supplementary Figure 1) had sufficient quality to trace the polypeptide chain except for the N-terminus and the loop region of the appendage. The model was built with TURBO-FRODO (Roussel and Cambillau, 1996) and refined to the resolutions of 3.1 Å by CNS (Brunger *et al*, 1998). The final model includes 210 residues (residues 26–71 and 84–247), and has an R factor of 23.6% (R_{free} of 26.4%). The ΔApp structure was solved by molecular replacement by MOLREP in the CCP4 suite (CCP4, 1994) and refined to the resolution of 2.9 Å by CNS. The simulated annealing omit electron density map calculated by CNS confirmed the continuous α-helical structure of the replaced region as designed (Supplementary Figure 7). The final model includes 200 amino-acid residues and has an R factor of 23.8% (R_{free} of 26.9%). The a4 mutant structure was solved by molecular replacement using the central core of the EndA1-BAR as a starting model and the arms were manually built (Supplementary Figure 7). The structure was refined to the resolution of 2.4 Å by CNS with an R factor of 21.5% (R_{free} of 26.9%). Main-chain dihedral angles of all non-glycine residues of these three models lie in allowed regions of the Ramachandran plot, with 94.3% for the EndA1-BAR, 94.1% for the ΔApp mutant, and 96.4% for the a4 mutant in most-favored regions, respectively. Graphical representations were prepared using the programs TURBO-FRODO, MOLSCRIPT (Kraulis, 1991), RASTER3D (Merritt and Bacon, 1997), GRASP (Nicholls *et al*, 1991) and Pymol (DeLano, 2002).

Liposome binding and tubulation assays

Liposome sedimentation assay and tubulation assay were as earlier described (Peter *et al*, 2004 see also McMahon lab protocols: http://www2.mrc-lmb.cam.ac.uk/NB/McMahon_H/group/techniqs/techniqs.htm) with slight modifications. Briefly, Folch fraction 1 (Sigma) was used as the lipid source and liposome suspension, 1 mg/ml in liposome buffer (20 mM HEPES, pH 7.4, 150 mM NaCl, 1 mM DTT) was made by sonication. Freshly purified BAR domain proteins were diluted at about 1 mg/ml in the liposome buffer and ultracentrifuged at 400 000 *g* for 10 min just before use. No crystallization occurred at this or lower concentrations. For sedimentation assays, 20 μg proteins were mixed with 25 or 75 μg liposomes in 100 μl of the liposome buffer, incubated for 10 min on ice and ultracentrifuged at 200 000 *g* for 10 min. For tubulation assays, 400 μg/ml proteins were mixed with an equal volume of 400 μg/ml liposomes, left for 10 s to 30 min at room temperature, and then processed for negative staining. Judging from the liposome sedimentation and the tryptophan fluorescence assays, this protein to lipid ratio ensured nearly saturated protein–liposome binding. Magnification was calibrated using a grating replica of 2160/mm.

Tryptophan fluorescence and FRET assay

Fluorescence emission spectra were recorded with a Hitachi F-4500 fluorescence spectrophotometer (Ohki *et al*, 2004). For tryptophan fluorescence assays, 140 μg/ml tryptophan-containing mutants were mixed with 0–200 μg/ml liposomes in the liposome buffer, incubated for 3 min, and excited at 280 nm. For FRET assays, DPH-liposomes were made by adding DPH (Molecular Probe) into lipid solution (1:500 to lipid, w:w). The fluorescence of DPH-liposomes (200 μg/ml) excited at 280 nm was scanned from 400 to 500 nm at 1-min intervals. The first measurement of the 430-nm DPH peak was obtained at about 30 s after mixing with mutant proteins (100 μg/ml).

Cell culture, transfection and surface biotinylation

HUVECs were purchased from Kurabo and cultured in HuMedia-EG2 as described previously (Sakurai *et al*., 2006). 293T cells, CHO cells, Cos7 cells, and NIH-3T3 cells were cultured in DMEM supplemented with 10% fetal bovine serum as described previously (Kamioka *et al*., 2004). Cells were transfected using LipofectAMINE 2000 (Invitrogen). Live HUVECs were biotinylated with 5 mM sulfo-NHS-biotin (Pierce) in Opti-MEM (Invitrogen) for 10 min. They were washed once with Opti-MEM and chased for 10 min with the normal culture medium, and fixed with 2% formaldehyde after a brief wash with Opti-MEM containing 1/20 volume of Avidin D blocking solution (Vector Laboratory) to reduce the cell surface background staining. HUVECs were permeabilized with cold MeOH and biotin was visualized using Alexa633-streptavidine (Molecular Probe).

Supplementary data

Supplementary data are available at *The EMBO Journal* Online.

Acknowledgements

We thank H Nakajima, T Matsu, Y Kawano and H Naitow for technical assistance with SPring-8 beamlines, and H Ago and M Miyano, Structural Biophysics Laboratory, RIKEN Harima Institute at SPring-8, for their helpful advice. This work was supported in part by Grant for Research on Advanced Medical Technology from the Ministry of Health, Labour, and Welfare of Japan, by the Program for Promotion of Fundamental Studies in Health Sciences of the National Institute of Biomedical Innovation (NIBIO), and by Special Coordination Funds for Promoting Science and Technology, Ministry of Education, Culture, Sports, Science and Technology (MEXT) of Japan.

Competing interests statement

The authors declare that they have no competing commercial interests in relation to this work.

References

Brunger AT, Adams PD, Clore GM, DeLano WL, Gros P, Grosse-Kunstleve RW, Jiang JS, Kuszewski J, Nilges M, Pannu NS, Read RJ, Rice LM, Simonson T, Warren GL (1998) Crystallography & NMR system: a new software suite for macromolecular structure determination. *Acta Crystallogr D* **54:** 905–921

Collaborative Computational Project Number 4 (1994) The CCP4 suite: programs for protein crystallography. *Acta Crystallogr D* **50:** 760–763

DeLano WL (2002) *The PyMOL User's Manual.* DeLano Scientific: San Carlos, CA, USA

Galli T, Haucke V (2004) Cycling of synaptic vesicles: How far? How fast!. *Sci STKE* **2004:** re19

Farsad K, Ringstad N, Takei K, Floyd SR, Rose K, De Camilli P (2001) Generation of high curvature membranes mediated by direct endophilin bilayer interactions. *J Cell Biol* **155:** 193–200

Farsad K, De Camilli P (2003) Mechanisms of membrane deformation. *Curr Opin Cell Biol* **15:** 372–381

Ford MG, Mills IG, Peter BJ, Vallis Y, Praefcke GJ, Evans PR, McMahon HT (2002) Curvature of clathrin-coated pits driven by epsin. *Nature* **419:** 361–366

Gallop JL, McMahon HT (2005) BAR domains and membrane curvature: bringing your curves to the BAR. *Biochem Soc Symp* **72:** 223–231

Habermann B. (2004) The BAR-domain family of proteins: a case of bending and binding. *EMBO Rep* **5:** 250–255

de Heuvel E, Bell AW, Ramjaun AR, Wong K, Sossin WS, McPherson PS (1997) Identification of the major synaptojanin-binding proteins in brain. *J Biol Chem* **272:** 8710–8716

Itoh T, Erdmann KS, Roux A, Habermann B, Werner H, De Camilli P (2005) Dynamin and the actin cytoskeleton cooperatively regulate plasma membrane invagination by BAR and F-BAR proteins. *Dev Cell* **9:** 791–804

Kamioka Y, Fukuhara S, Sawa H, Nagashima K, Masuda M, Matsuda M, Mochizuki N. (2004) A novel dynamin-associating molecule, formin-binding protein 17, induces tubular membrane invaginations and participates in endocytosis. *J Biol Chem* **279:** 40091–40099

Karbowski M, Jeong SY, Youle RJ (2004) Endophilin B1 is required for the maintenance of mitochondrial morphology. *J Cell Biol* **166:** 1027–1039

Kraulis PJ (1991) MOLSCRIPT: a program to produce both detailed and schematic plots of protein structure. *J Appl Crystallogr* **24:** 946–950

McMahon HT, Mills IG (2004) COP and clathrin-coated vesicle budding: different pathways, common approaches. *Curr Opin Cell Biol* **16:** 379–391

McMahon HT, Gallop JL (2005) Membrane curvature and mechanisms of dynamic cell membrane remodeling. *Nature* **438:** 590–596

Merritt EA, Bacon DJ (1997) Raster3D: photorealistic molecular graphics. *Methods Enzymol* **277:** 505–524

Modregger J, Schmidt AA, Ritter B, Huttner WB, Plomann M (2003) Characterization of Endophilin B1b, a brain-specific membrane-associated lysophosphatidic acid acyl transferase with properties distinct from endophilin A1. *J Biol Chem* **278:** 4160–4167

Nicholls A, Sharp K, Honig B (1991) Protein folding and association: insights from the interfacial and thermodynamic properties of hydrocarbons. *Proteins* **11:** 281–296

Nossal R, Zimmerberg J (2002) Endocytosis: curvature to the ENTH degree. *Curr Biol* **12:** R770–R772

Ohki T, Mikhailenko SV, Morales MF, Onishi H, Mochizuki N (2004) Transmission of force and displacement within the myosin molecule. *Biochemistry* **43:** 13707–13714

Otwinowski Z, Minor W (1997) Processing of X-ray diffraction data collected in oscillation mode. *Methods Enzymol* **276:** 307–326

Peter BJ, Kent HM, Mills IG, Vallis Y, Butler PJ, Evans PR, McMahon HT (2004) BAR domains as sensors of membrane curvature: the amphiphysin BAR structure. *Science* **303:** 495–499

Repáková J, Holopainen JM, Morrow MR, McDonald MC, Capkova P, Vattulainen I (2005) Influence of DPH on the structure and dynamics of a DPPC bilayer. *Biophys J* **88:** 3398–3410

Ringstad N, Nemoto Y, De Camilli P (1997) The SH3p4/Sh3p8/SH3p13 protein family: binding partners for synaptojanin and dynamin via a Grb2-like Src homology 3 domain. *Proc Natl Acad Sci USA* **94:** 8569–8574

Ringstad N, Nemoto Y, De Camilli P (2001) Differential expression of endophilin 1 and 2 dimers at central nervous system synapses. *J Biol Chem* **276:** 40424–40430

Roussel A, Cambillau C (1996) *TURBO-FRODO Manual.* Marseille France AFMB-CNRS, Paris, France

Sakurai A, Fukuhara S, Yamagishi A, Sako K, Kamioka Y, Masuda M, Nakaoka Y, Mochizuki N (2006) MAGI-1 is required for Rap1 activation upon cell–cell contact and for enhancement of vascular endothelial cadherin-mediated cell adhesion. *Mol Biol Cell* **17:** 966–976

Schuske KR, Richmond JE, Matthies DS, Davis WS, Runz S, Rube DA, van der Bliek AM, Jorgensen EM (2003) Endophilin is required for synaptic vesicle endocytosis by localizing synaptojanin. *Neuron* **40:** 749–762

Tarricone C, Xiao B, Justin N, Walker PA, Rittinger K, Gamblin SJ, Smerdon SJ (2001) The structural basis of Arfaptin-mediated cross-talk between Rac and Arf signalling pathways. *Nature* **411:** 215–219

Terwilliger TC (1999) Reciprocal-space solvent flattening. *Acta Crystallogr D* **55:** 1863–1871

Terwilliger TC, Berendzen J (1999) Automated MAD and MIR structure solution. *Acta Crystallogr D* **55:** 849–861

Verstreken P, Koh TW, Schulze KL, Zhai RG, Hiesinger PR, Zhou Y, Mehta SQ, Cao Y, Roos J, Bellen HJ (2003) Synaptojanin is recruited by endophilin to promote synaptic vesicle uncoating. *Neuron* **40:** 733–748

Weissenhorn W (2005) Crystal structure of the endophilin-A1 BAR domain. *J Mol Biol* **351:** 653–661

Wenk MR, De Camilli P (2004) Protein-lipid interactions and phosphoinositide metabolism in membrane traffic: insights from vesicle recycling in nerve terminals. *Proc Natl Acad Sci USA* **101:** 8262–8269

Yamagishi A, Masuda M, Ohki T, Onishi H, Mochizuki N (2004) A novel actin-bundling/filopodium-forming domain conserved in insulin receptor tyrosine kinase substrate p53 and missing in metastasis protein. *J Biol Chem* **279:** 14929–14936

Zimmerberg J, Kozlov MM (2006) How proteins produce cellular membrane curvature. *Nat Rev Mol Cell Biol* **7:** 9–19

Cardiac Ischemia Activates Vascular Endothelial Cadherin Promoter in Both Preexisting Vascular Cells and Bone Marrow Cells Involved in Neovascularization

Naoko Kogata, Yuji Arai, James T. Pearson, Kazuaki Hashimoto, Kyoko Hidaka, Tatsuya Koyama, Satoshi Somekawa, Yoshikazu Nakaoka, Minetaro Ogawa, Ralf H. Adams, Masato Okada, Naoki Mochizuki

Abstract—Vascular endothelial cadherin (VE-cadherin) is expressed on vascular endothelial cells, which are involved in developmental vessel formation. However, it remains elusive how VE-cadherin–expressing cells function in postnatal neovascularization. To trace VE-cadherin–expressing cells, we developed mice expressing either green fluorescent protein or LacZ driven by VE-cadherin promoter using Cre-loxP system. Although VE-cadherin promoter is less active after birth than during embryogenesis in blood vessels, it is reactivated on cardiac ischemia. Both types of reporter-positive cells are found in the vasculature and in the infarcted myocardium. Those found in the vasculature were pre-existing endothelial cells and incorporated endothelial progenitor cells derived from extracardiac tissue. In addition to the vasculature, VE-cadherin promoter-activated cells were positive for CD45 in the bone marrow cells of the infarcted mice. VE-cadherin promoter–reactivated CD45-positive leukocytes were also found in the infarcted area. In addition, VE-cadherin promoter was activated in the bone marrow vessels of the infarcted mice. Collectively, our findings reveal a new ischemia-induced neovascularization mechanism involving VE-cadherin; the re-expressed VE-cadherin–mediated cell adhesion between cells may be involved not only in homing of bone marrow–derived cells to ischemic area but also mobilization from bone marrow. (***Circ Res.* 2006;98:897-904.**)

Key Words: vasculogenesis ■ angiogenesis ■ hemangioblast ■ ischemia ■ CD45

Cell-based therapies have been aimed at neovascularization in ischemic diseases.[1] Recruitment of both angiogenic factor-producing hematopoietic cells and vasculature-constituting endothelial cells to the ischemic area contributes to neovascularization.[2] Endothelial progenitor cells (EPCs) and circulating bone marrow–derived EPCs (CEPCs) are incorporated into the nascent vessels.[3,4] These cells have been suggested to originate from bone marrow. On the basis of this potential differentiation capability, bone marrow cell–based therapy has been attempted and proven to be effective for ischemic heart disease and peripheral artery disease.[5,6] However, it is unclear how bone marrow–derived cells are recruited to the ischemic area.

Postnatal neovascularization includes angiogenesis and vasculogenesis. Both steps cooperatively work by involving the sprouting and branching of the pre-existing endothelial cells and recruiting EPCs in the vascular tree.[7] Proangiogenic factors released from ischemic tissue and infiltrating cells, including vascular endothelial growth factor (VEGF), fibroblast growth factor, granulocyte macrophage colony-stimulating factor, and placental growth factor, mobilize hematopoietic stem cells (HPCs) as well as EPCs to the infarcted area.[8–10] Thus, HPCs and EPCs homing to the ischemic area are involved in angiogenesis and vasculogenesis in coordination with pre-existing vascular cells. Similar to adult neovascularization, embryonic vasculogenesis and angiogenesis are coordinated by both endothelial lineage cells and hematopoietic cells originating from hemangioblasts.

Several cell surface molecules, including CD133, VEGF receptor 2, vascular endothelial cadherin (VE-cadherin), and CD34, have been used to characterize the EPCs in the bone marrow and CEPCs in the peripheral blood.[6] Although the cells purified by cell surface marker have been demonstrated to be recruited to the ischemic area when transferred for cell-based therapy, it is elusive how and what endogenous EPCs, CEPCs, and HPCs are mobilized to ischemic area for neovascularization in ischemic diseases.

VE-cadherin (Cadherin5, CD144), which belongs to cadherin super family, is expressed on cultured vascular endothelial cells and is essential for endothelial cell–cell interaction.[11] Whereas N-cadherin, another cadherin expressed on the endothelial cells, is thought to function in adherens

Original received April 20, 2005; revision received February 28, 2006; accepted March 8, 2006.

From the Departments of Structural Analysis (N.K., Y.N., T.K., S.S., N.M.), Bioscience (Y.A., K.H.), and Cardiac Physiology (J.T.P.); National Cardiovascular Center Research Institute, Osaka, Japan; the Department of Cell Differentiation, Institute for Molecular Embryology and Genetics (K.H., M.O.), Kumamoto University, Kumamoto, Japan; the Vascular Development Laboratory (R.H.A.), Cancer Research UK London Research Institute, United Kingdom; and the Department of Oncogene Research (M.O.), Institute for Microbial Disease, Osaka University, Japan.

Correspondence to Naoki Mochizuki, Department of Structural Analysis, National Cardiovascular Center Research Institute, 5-7-1 Fujishirodai, Suita, Osaka 565-8565, Japan. E-mail nmochizu@ri.ncvc.go.jp

Circulation Research is available at http://circres.ahajournals.org DOI: 10.1161/01.RES.0000218193.51136.ad

junctions between endothelial cells and mural cells (pericytes and vascular smooth muscle cells [VSMCs]).[12] VE-cadherin is required in vivo in the postnatal vasculature to maintain endothelial cell integrity and barrier function.[13,14] Moreover, VE-cadherin associated with VEGF receptor is involved in the regulation of permeability after myocardial ischemia.[15]

In the present study, we investigated the role of VE-cadherin promoter-activated cells in ischemia-induced neovascularization. We demonstrate that VE-cadherin promoter is activated in the pre-existing vascular endothelial cells of bone marrow and heart. In addition, we noticed VE-cadherin promoter is activated in the bone marrow cells and peripheral blood cells presumably corresponding to EPCs/CEPCs and CD45-positive cells preferentially homing to infarcted heart. Thus, we raise the possibility of VE-cadherin–mediated cell–cell contact for effective homing of proangiogenic cells to ischemic tissues.

Materials and Methods

Generation of Transgenic Mice

Cre recombinase driven by VE-cadherin promoter (VE-cad-Cre) mice contained the 4.2-kb VE-cad-Cre transgene (Figure 1A) excised from pBluescript-VE-cad-Cre (online supplement, available at http://circres.ahajournals.org). VE-cad-Cre mice were crossed with LacZ reporter mice (cAct-XstopX-LacZ from the Jackson Laboratory, Bar Harbor, Me) or enhanced green fluorescent protein (GFP) reporter mice (CAG-CAT–enhanced GFP [EGFP] obtained from J. Miyazaki, Osaka University).[16] The offspring were named VE-cadherin promoter-driven LacZ-expressing mice (VE/Z) and VE-cadherin promoter-driven EGFP-expressing mice (VE/EG), respectively. All animal experiments were approved by the animal committee of the National Cardiovascular Center and performed according to the regulation of the National Cardiovascular Center.

Detection of Fluorescence In Vivo

VE/EG embryos and dissected organs from VE/EG mice were examined using an Olympus SZX12 stereo-fluorescent microscope equipped with a VB-6010 charge-coupled device camera. The organs from control mice were imaged next to those from VE/EG mice.

Histochemistry, Immunostaining, Immunofluorescence, and In Situ Hybridization

The procedures of histological examination are described in the online supplement.

Neovascularization Models

To monitor VE-cadherin promoter–activated cells during neovascularization, we used a corneal angiogenesis model of 8-week-old VE/EG mouse and myocardial infarction model. Both methods are described in the online supplement.

Parabiosis Model

Pairs of a 6- to 10-week-old wild-type and VE/Z mice were subjected to parabiotic surgery. Mice were surgically joined from shoulder to femur. One week after parabiotic surgery, the coronary artery was ligated in the wild-type mouse.

Characterization of EGFP-Expressing Cells by Flow Cytometric Analysis

EGFP expression of these cells was analyzed by FACS (fluorescence-activated cell sorting) Calibur (BD Biosciences). EGFP together with cell surface antigen immunostained with phycoerythrin-conjugated anti-CD31 or anti-CD45 were investigated using FACS VantageSE or FACS Aria (BD Biosciences).

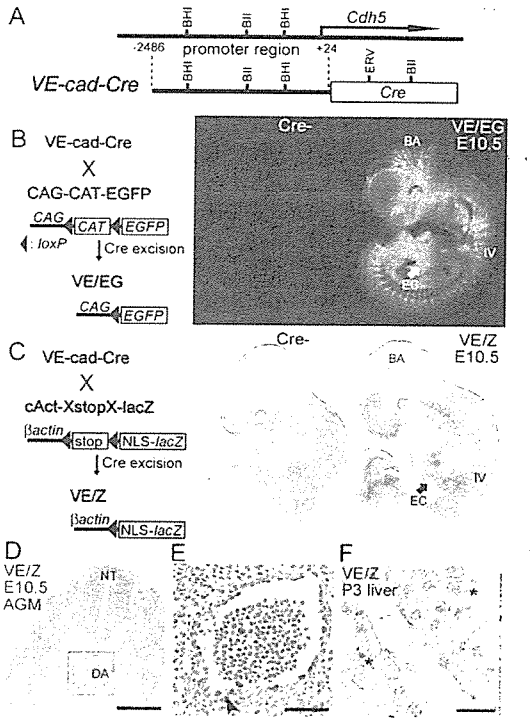

Figure 1. VE-cadherin (Cadherin5, Cdh5) promoter is activated during developmental vascularization. A, VE-cadherin promoter-driven Cre recombinase expressing mouse. BHI, Bam HI; BII, BglII; ERV, EcoRV. B, VE-cadherin promoter-dependent EGFP-expressing mouse (VE/EG). EGFP was expressed in intersomitic vessels (IV), and basilar artery (BA), and endocardium (EC) of VE/EG mice at embryonic day 10.5 (E10.5). No EGFP expression in a littermate lacking *Cre* gene (Cre-). C, VE-cadherin–dependent LacZ-expressing mouse (VE/Z). Whole-mount X-gal staining of E10.5 VE/Z mice shows similar reporter expression to VE/EG. NLS indicates nuclear localization signal. D, Cross-section of neural tube, dorsal aorta, and somites of E10.5 VE/Z embryo shows LacZ-positive signals in dorsal aorta (DA). Bar=200 μm. E, Box in D is enlarged. LacZ-positive cells are present in the hematopoietic cells in the dorsal aorta lumen and its lining cells (arrowhead). Bar=50 μm. F, In the liver, LacZ-expressing cells are detected in the sinusoidal endothelium and the scattered cells, which seem to be hematopoietic cells (asterisks). Bar=20 μm.

Results

VE-Cadherin Promoter Is Activated in Cells Responsible for Developmental Vessel Formation

To trace the VE-cadherin–expressing cells in fetal vascular development and postnatal neovascularization, we first generated transgenic mice expressing VE-cad-Cre (Figure 1A). By crossing three lines of VE-cad-Cre mice with either EGFP reporter mice or LacZ reporter mice, we obtained VE/EG and VE/Z (Figure 1B and 1C).

EGFP and LacZ expression by VE-cad-Cre–mediated recombination was observed in embryonic vascular development (Figure 1B and 1C). We examined LacZ expression in Aorta-Gonad-Mesonephros (AGM) region of VE/Z mice where hemangioblasts reside.[17,18] LacZ-positive cells were detected in the dorsal aorta (Figure 1D, boxed). We noticed that LacZ-stained cells were in the lumen and in the lining cells of the ventral wall (Figure 1E, arrowhead) and in the cells that seemed to bud off from the inner layer. LacZ-

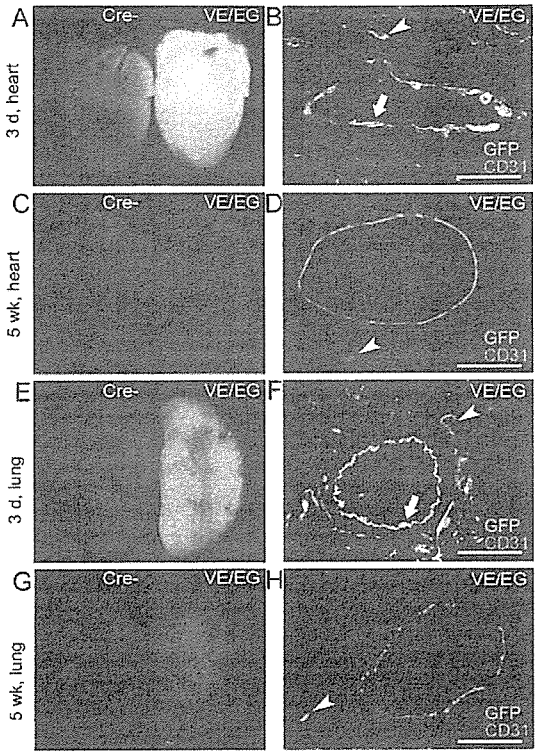

Figure 2. VE-cadherin promoter is less activated after birth than before birth. Organs from littermates lacking *Cre* gene (Cre-) do not show any EGFP expression (A, C, E, and G). A, EGFP is observed in the heart of newborn (3 days after birth) VE/EG mice. B, In the section of a newborn VE/EG mouse heart, EGFP is detected by anti-GFP (green) among the CD31-positive (red) arterial vascular endothelial cells (arrow) and capillary endothelial cells (arrowhead). Positive immunoreaction for anti-GFP and anti-CD31 is visualized by Alexa488-conjugated goat anti-rabbit antibody (green) and Alexa 546-conjugated anti-mouse antibody (red), respectively. C, EGFP is not expressed in the 5-week-old VE/EG mouse heart. D, A few EGFP-positive cells (arrowhead) are detected in capillaries of 5-week-old VE/EG mice. E, Similar to the heart, EGFP is observed in the newborn VE/EG mouse lung. F, EGFP (green) is merged with CD31-positive (red) arterial endothelial cells (arrow) and capillary endothelial cells (arrowhead). G, Lungs of 5-week-old VE/EG mice do not express EGFP. H, A few EGFP-positive cells (arrowhead) were detected in capillaries of the VE/EG mouse lung. Bar=50 μm.

stained cells were also found in the newborn VE/Z mouse liver, where hepatic hematopoiesis is organized (Figure 1F, asterisks). These results suggest that VE-cadherin promoter is activated in the cells probably corresponding to hemangioblasts responsible for fetal vasculogenesis.

VE-Cadherin Promoter Becomes Less Active After Birth

To assess the involvement of VE-cadherin in postnatal vascular development, we examined changes in EGFP reporter expression with age in tissues. Although EGFP expression in both neonatal heart and lung was noticeable, its expression was gradually decreased by aging and no longer observed by the fifth week (Figure 2A, 2C, 2E, and 2G). EGFP and CD31 (platelet and endothelial cell adhesion molecule-1) expression overlapped in the vascular endothelium of both heart and lung of the neonatal VE/EG mice, as revealed by immunohistochemical analyses using anti-GFP

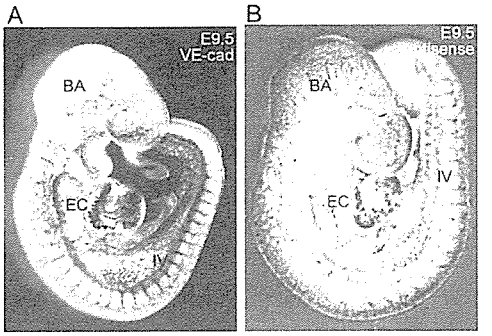

Figure 3. VE-cadherin expression and VE-cadherin mRNA expression in embryogenesis. A, VE-cadherin is detected in the basilar arteries (BA), endocardium (EC), and intersomitic vessels (IV) by immunohistochemistry in an embryonic 9.5 (E9.5) wild-type mouse embryo using anti–VE-cadherin antibody. B, In situ hybridization using antisense probe for VE-cadherin mRNA reveals that VE-cadherin mRNA is expressed in BA, EC, and IV of an E9.5 wild-type mouse embryo. Sense probe used as a negative control does not detect any VE-cadherin mRNA (data not shown). Bar=50 μm.

and anti-CD31 antibodies (Figure 2B and 2F). In clear contrast, GFP was not detected in the CD31-positive vascular endothelium of 5-week-old VE/EG mice (Figure 2D and 2H). Similarly, we found that EGFP expression was decreased with age in other organs, including the brain, liver, and kidney (data not shown).

Tie2 is a tyrosine kinase receptor for angiopoietin and is expressed in the endothelial cells and hematopoietic cells.[19] Thus, we further compared the VE-cadherin promoter-dependent EGFP expression with that dependent on Tie2 promoter. EGFP expression persisted through the entire life (supplemental Figure II), supporting that the VE-cadherin promoter is more active during embryonic and prenatal vascularization than postnatal vessel maintenance. Similarly, VE-cadherin promoter-driven LacZ expression was decreased with aging (supplemental Figure II).

VE-Cadherin Is Expressed in Developing Vasculature

To confirm that VE-cadherin promoter-driven EGFP and LacZ reporter expression reflects endogenous VE-cadherin expression in vivo, we examined the expression of VE-cadherin and VE-cadherin mRNA in embryo. VE-cadherin, VE-cadherin mRNA was detected in developing vessels of the embryo stained with anti–VE-cadherin antibody (Figure 3A) and of the embryo probed with antisense–VE-cadherin cDNA (Figure 3B). VE-cadherin protein and VE-cadherin mRNA were detected in the basilar arteries, intersomitic vessels, and endocardium as reporters of VE/EG and VE/Z mice were expressed. These results indicate that VE-cadherin promoter-driven reporter expression of both VE/EG and VE/Z mice reflects the endogenous VE-cadherin expression.

VE-Cadherin Promoter-Activated Cells Are Involved in Neovascularization

EPCs are positive for VE-cadherin and involved in neovascularization.[6] We hypothesized that VE-cadherin promoter is turned on in EPCs during adult vasculogenesis and that VE-cadherin promoter may be reactivated in vessels. There-

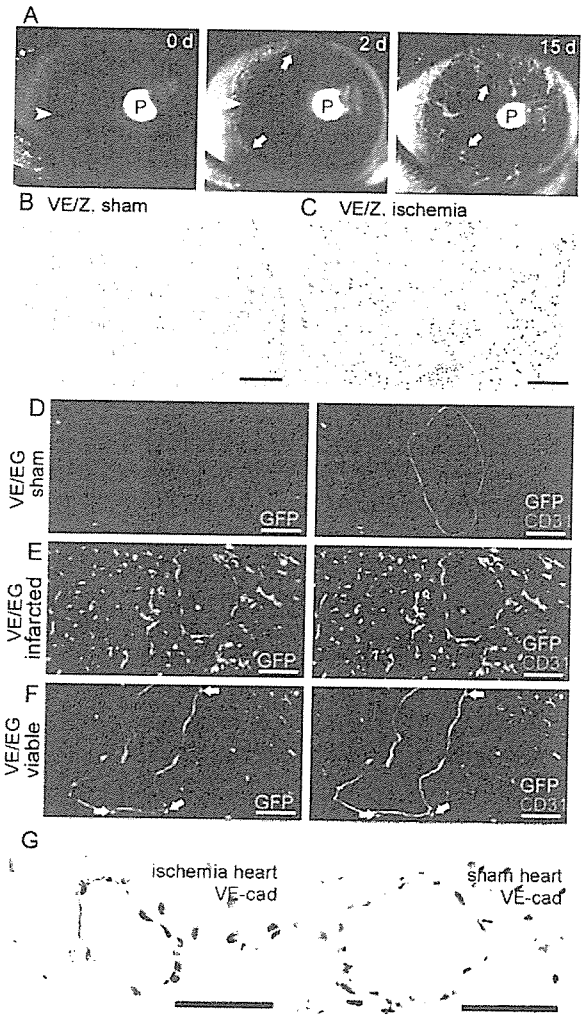

Figure 4. Reactivation of VE-cadherin promoter in response to VEGF and cardiac ischemia. A, New vessel formation monitored by EGFP expression in the VE/EG mouse cornea just 0 days (0 d), 2 days (2 d), and 15 days (15 d) after the implantation of a VEGF-containing pellet (P). Arrowheads and arrows denote the limbus vessels and nascent vessels, respectively. B, Section of sham coronary-ligated VE/Z mouse shows no LacZ-stained cells in the heart. Bar=100 μm C, Numerous LacZ-stained cells are present in the infarcted region of the VE/Z mouse 3 days after coronary ligation. Bar=100 μm. D, The section of the sham-operated VE/EG mouse heart was immunostained with anti-GFP and anti-CD31. Similar to Figure 2, Alexa488 image and that merged with Alexa546 image are shown in the left and right panels, respectively. E, Immunostaining similar to D shows partial colocalization of GFP (green) and CD31 (red) in the infarcted area of VE/EG mouse heart. F, Colocalization of GFP (green) and CD31 (red) in the both arteries and capillaries in the viable area surrounding the infarcted area. Arrowheads denote the GFP-positive cells outside of the endothelium and inside of vascular wall. Bars (in D, E, and F)=50 μm. G, VE-cadherin is detected (brown) in the vessels of infarcted heart but not sham-operated heart. Bar=25 μm.

fore, we first tested whether VEGF induces EGFP expression in using a cornea model of VE/EG mice. After implanting VEGF-containing pellets, EGFP expression was monitored every day. Not only new vessels growing toward the implanted pellets but also limbus vessels exhibited EGFP expression (Figure 4A), indicating that VE-cadherin promoter is activated in the vascular cells involved in neovascularization.

We next tested whether ischemia triggers VE-cadherin expression in a myocardial infarction model. When the coronary artery of VE/Z mice was ligated, LacZ-positive cells were found 3 days after coronary ligation in the hearts of the infarcted mice but not those in the sham-operated mice (Figure 4B and 4C). Similarly, EGFP expression was examined by immunohistochemistry using anti-GFP antibody. In sham-operated control VE/EG mice, GFP-positive cells were not detected in the heart except a few capillaries (Figure 4D), whereas GFP-positive cells were observed in the infarcted area (Figure 4E, left). Notably, among GFP-positive cells, we found CD31-positive cells in the merged image (Figure 4E, right). More than 50% of GFP-positive cells were negative for CD31, suggesting that GFP-positive cells may include nonendothelial lineage cells. Intriguingly, the endothelial cells lining the vessels marked by CD31 in the adjacent viable region were positive for GFP (Figure 4F). In addition, we could find GFP-positive cells in the nonendothelial cell layer in the arterial walls, probably smooth muscle cell layer in the viable area (Figure 4F, arrows). Consistent with GFP reporter expression, VE-cadherin was detected by immunohistochemistry in the endothelium and smooth muscle cells in the vessels of the infarcted heart but not in the sham-operated heart (Figure 4G).

Ischemia Triggers VE-Cadherin Expression in Preexisting Vascular Cells and Mobilized Cells

To test whether the VE-cadherin promoter-activated cells are derived from extracardiac tissues of infarcted mice, we used a parabiotic pairing between a wild-type mouse and a VE/Z mouse (Figure 5, gray mouse and blue mouse, respectively). In a parabiotic mice model, circulating blood cells are mixed through vascular anastomoses that form between the two mice.[20,21] LacZ-positive cells were found in both endothelial cell layer and smooth muscle cell layer of infarcted VE/Z mouse (Figure 5A, arrowhead and arrow, respectively), as confirmed by the same section immunostained with anti-CD31 and anti-α-smooth muscle actin (SMA). In a parabiosis model in which the wild-type mouse was coronary ligated (indicated by cross), we observed that LacZ-positive cells were recruited to the infarcted area of the wild-type mouse (Figure 5B, denoted by cross) from the VE/Z mice (Figure 5B, left). These results indicate that VE-cadherin promoter-reactivated cells are derived from extracardiac tissues and subsequently home to the infarcted heart. Notably, these LacZ-stained cells were negative for CD31 or α-SMA (Figure 5B, right). These results were consistent with those found in the infarcted area of VE/EG mice (Figure 4E). In addition to the infarcted area, LacZ-positive cells were incorporated in the vascular endothelial cell layer and VSMC layer of the viable area (Figure 5C and D), although the number of LacZ-positive cells were much less than that of unconnected mouse. Given that most of the endothelial cells lining the vessels of viable area of infarcted VE/EG mice were positive for GFP (Figure 4E) and that the number of LacZ-positive cells found in the vessels were much less in parabiotic model, VE-cadherin promoter is activated in the pre-existing vessels

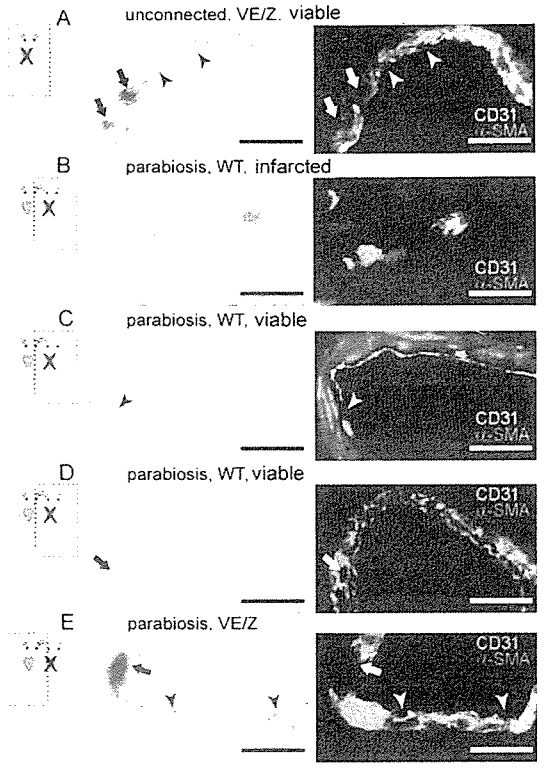

Figure 5. Ischemia induces the recruitment of circulating VE-cadherin promoter-activated cells. Sections show tissues for the mouse indicated by the broken line box. In all panels, crosses indicate coronary ligation, and arrowheads and arrows denote LacZ/CD31-positive and LacZ/α-SMA–positive cells, respectively. All images were obtained by a confocal microscope (LSM510 META; Carl Zeiss). A, LacZ-stained cells in both α-SMA–positive cell layer and CD31-positive cell layer in the arteries of the viable area of infarcted VE/Z mice (cross). B, C, D, and E, A parabiotic pairing between a wild-type (WT) mouse (gray) and a VE/Z mouse (blue). B, Sections of the infarcted heart region of the wild-type mouse were examined for LacZ expression. LacZ-positive cells are negative for CD31 and α-SMA. C and D, In the same model as B, LacZ expression was examined in variable area of infarcted wild-type mouse. E, Coronary arteries of the noninfarcted VE/Z mouse were examined for LacZ expression. Bars=10 μm.

of viable area. Collectively, these data indicate that VE-cadherin–expressing cells, which do not correspond to vascular cells, are recruited to infarcted area from extracardiac tissue. Notably, when examining the heart of the donor VE/Z mouse without myocardial infarction, LacZ-stained cells were found in both endothelial cell layer and VSMC layer in spite of the absence of cardiac ischemia (Figure 5E), indicating that circulating stimuli may activate VE-cadherin promoter in either the pre-existing vascular cells or the mobilized cells from extracardiac tissue to the vasculature. Parabiosis itself did not trigger LacZ expression before the ischemia (supplemental Figure IIIA). Cardiac ischemia, not but other organ ischemia, is critical for VE-cadherin expression in the heart (supplemental Figure III).

VE-Cadherin Promoter Is Activated in Bone Marrow Cells and Circulating Blood Cells on Myocardial Ischemia

To investigate the origin of the cells homing to the ischemic tissues from extracardiac tissue, we explored EGFP-expressing cells in bone marrow and peripheral blood of the infarcted VE/EG mice by flow cytometry. Although EGFP-expressing cells were not detected in the bone marrow of the sham-operated mice, EGFP-expressing bone marrow cells increased after coronary ligation and reached 5% of total bone marrow mononuclear cells (Figure 6A and 6B). In parallel with the increase of EGFP-expressing cells in bone marrow, EGFP-expressing cells also increased in the peripheral blood (Figure 6C). No EGFP-expressing cells were detected in the blood from sham-operated mice. EGFP-expressing cells increased up to 6% of total circulating mononuclear cells 7 days after ligation (Figure 6D).

EGFP-expressing cells were observed in situ in the vasculature as well as in the marrow cells of infarcted VE/EG mice (Figure 6F) but not in sham-operated mice (Figure 6E), suggesting that VE-cadherin–mediated cell adhesion may be involved in mobilization of bone marrow cells into the bloodstream.

We further examined the expression of endogenous VE-cadherin in the EGFP-expressing cells sorted from the bone marrow of infarcted VE/EG mice. More than 90% and 40% of EGFP-expressing cells were positive for VE-cadherin and for CD31, respectively (Figure 6G and 6H). These data indicate that EGFP reporter expression reflects endogenous VE-cadherin expression in bone marrow cells. To characterize the CD31-negative cells, we performed flow cytometric analysis on mononuclear bone marrow cells obtained from infarcted VE/EG mice 2 days after coronary ligation using anti-CD31 and anti-CD45 because CD45 is expressed in the common origin of both myeloid cells and endothelial cells.[5] Among EGFP-positive cells, 50% were positive for CD31, in agreement with the immunostaining of GFP-positive cells with anti-CD31 (Figure 6H and 6I). Of note, all EGFP-expressing cells were positive for the pan-leukocyte cell marker CD45. VE-cadherin mRNAs of bone marrow CD45-positive cells of infarcted mice were twice as much as those of sham-operated mice (supplemental Figure V). These results indicate that EGFP-expressing cells consist of either multilineage cells or distinct stages of differentiated cell from a common origin: CD45-positive EPCs, CD45-positive hematopoietic precursor cells, and CD45-positive hematopoietic cells.

VE-Cadherin Promoter-Activated CD45-Positive Cells Are Actively Recruited to Ischemic Area

We found that VE-cadherin promoter-activated cells were positive for CD45 (Figure 6I) and that CD31-negative GFP-expressing cells were detected in the infarcted area (Figure 4E). Thus, we assumed that CD31-negative GFP-expressing cells might be CD45-positive cells in the infarcted heart. The heart of the infarcted VE/EG mice were immunostained with anti-GFP and anti-CD45. Double-positive staining was found in cells other than elongated cells that seemed to be endothelial cells (Figure 7A). The percentage of double-positive cells among CD45-positive cells in the infarcted area (>10% of CD45-positive cells were positive for GFP) was greater than that of CD45/EGFP-expressing cells in bone marrow cells as examined by FACS analysis (≈1.5% of CD45-positive cells were GFP positive; Figure 6I), indicating that double-positive

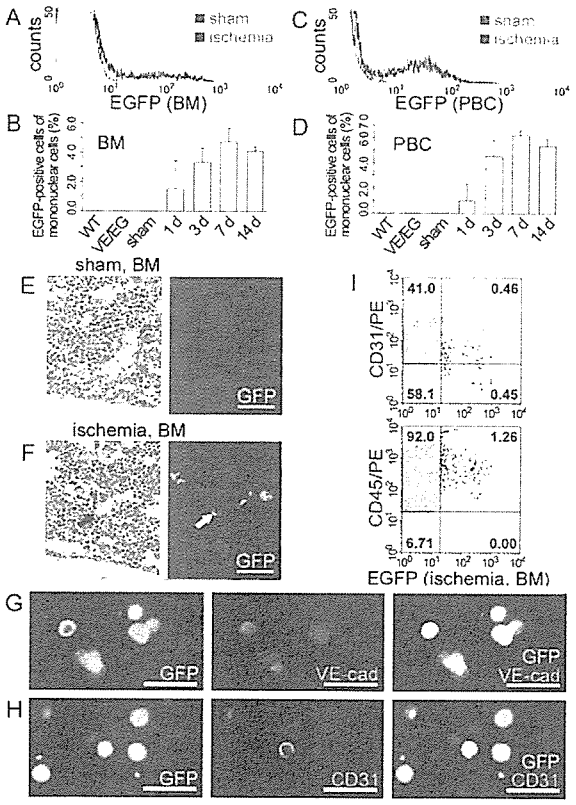

Figure 6. Ischemia induces increases in VE-cadherin promoter-activated bone marrow cells and blood cells. A, Flow cytometric analysis reveals EGFP-expressing cells appearing in bone marrow (BM) 3 days after coronary artery ligation in a VE/EG mouse (green) but not in a sham-operated VE/EG mouse (gray). B, EGFP-expressing cells in bone marrow cells obtained from the infarcted VE/EG mice were counted by flow cytometry. WT indicates wild-type mice; VE/EG, VE/EG mice without any operation; sham, sham-operated VE/EG mice; 1 d, 3 d, 7 d, and 14 d; 1 day, 3 days, 7 days, and 14 days after coronary ligation of VE/EG mice, respectively (n=3). C, Similar to A, EGFP-expressing cells increased in peripheral blood cells (PBC) of the coronary-ligated VE/EG mouse (green) but not in the sham-operated mouse (gray). D, Similar to B, EGFP-expressing peripheral blood cells obtained from infarcted mice were analyzed by flow cytometry. E, Expression of VE-cadherin in BM of sham-operated VE/EG mouse examined by immunostaining with anti-GFP. F, Similar to E, VE-cadherin promoter-reactivated cells were examined in the infarcted VE/EG mouse BM. Arrowheads indicate the immunopositive signal (green) in the endothelium of vessels. Bar=50 μm. G, EGFP-expressing cells obtained by cell sorting from the BM of VE/EG mouse 3 days after coronary ligation were immunostained with anti-GFP (left) and anti–VE-cadherin (center). The GFP image (green) and VE-cadherin image (red) is merged (right). A representative result of more than three independent experiments is shown. H, EGFP-expressing cells obtained from the same mouse as in G were immunostained with anti-GFP (left) and anti-CD31 (center). The merged image is shown in the right panel. I, Bone marrow cells obtained from an infarcted VE/EG mouse 2 days after coronary ligation were immunostained with phycoerythrin (PE)-conjugated anti-CD31 (top) or PE-conjugated anti-CD45 (bottom) and subjected to FACS analysis. Numbers indicate the percentage of cells in the fraction. A representative result of more than three independent experiments is shown.

cells were more selectively recruited to the ischemic area than single CD45-positive cells.

Discussion

Here we show for the first time that VE-cadherin promoter-activated cells are detected in both bone marrow cells and

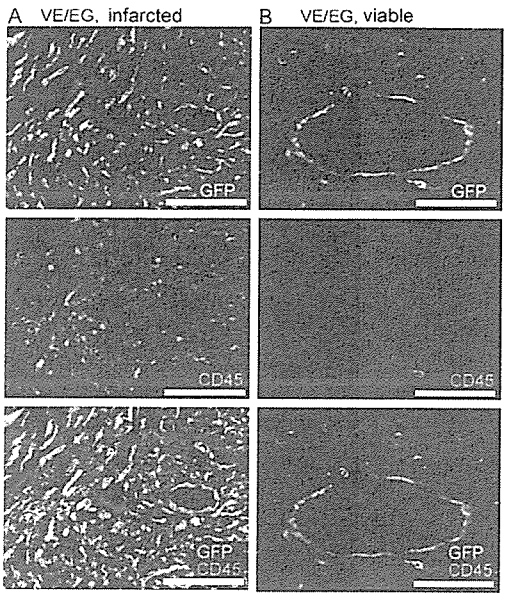

Figure 7. VE-cadherin promoter-activated CD45-positive cells after cardiac ischemia migrate to the infarcted area. A, The infarcted area of the mouse heart immunostained with anti-GFP (top) and anti-CD45 (middle). The GFP image and the CD45 image are merged (bottom). B, The viable area of the same mouse heart was also immunostained with anti-GFP (top), anti-CD45 (middle), and merged (bottom). Bar=100 μm.

blood vessels in the infarcted mice. Although VE-cadherin promoter is less active with aging, reactivated VE-cadherin promoter drives VE-cadherin expression in the pre-existing vessels of ischemic hearts. Our results do not suggest that VE-cadherin is not expressed in mature vessels but rather suggests that VE-cadherin expression is enhanced during ischemia, as detected by anti–VE-cadherin antibody (Figure 4G). Although VE-cadherin is required in the postnatal vascular endothelial cell integrity,[13,14] VE-cadherin is hardly detectable by immunohistochemistry.[22] Ischemia may drive VE-cadherin promoter, resulting in detectable increased VE-cadherin expression in the pre-existing vessels.

What is the role of re-expressed VE-cadherin of the vascular vessels during ischemia? VE-cadherin expression during ischemia may make conditions favorable for the homing of EPCs/CEPCs and the integration of these cells to create the neovessels. VE-cadherin may function not only as an endothelial cell–cell adhesion molecule, but as a leukocyte–endothelial cell adhesion molecule. Leukocytes extravasate across the endothelial cell layer via homophilic platelet and endothelial cell adhesion molecule-1 (CD31), binding between leukocytes and vascular endothelial cells because leukocytes do not express VE-cadherin.[23,24] Because VE-cadherin promoter was activated in CD45-positive leukocytes on ischemia, VE-cadherin on both pre-existing vessels and CD45-positive cells may help to the extravasation of CD45-positive cells.

We noticed that ischemia induced VE-cadherin promoter activation of both marrow cells and endothelium in the bone (Figure 6F). In addition, VE-cadherin promoter-activated marrow cells were positive for VE-cadherin (Figure 6G).VE-cadherin re-expression induced by ischemia appears to pro-

mote the mobilization of VE-cadherin–expressing cells from bone marrow because VE-cadherin regulates the mobilization of bone marrow cells across bone marrow endothelium.[25] Angiopoietin-1/Tie2 signaling maintains an HPC quiescence in bone marrow, probably by regulating N-cadherin.[26] Thus, ischemia may trigger the cadherin switch from N-cadherin to VE-cadherin in cells mobilizing from the bone marrow niche. These CD45-positive cells may function as proangiogenic factor-producing cells at the ischemic tissue.

VE-cadherin may be expressed in both prenatal and postnatal hemangioblasts. In embryos and embryonic stem cells, VE-cadherin–expressing cells have the potential to generate hematopoietic precursors,[27–29] which exist and repopulate in the AGM to differentiate into both hematopoietic cells and endothelial cells.[17] Consistently, we found LacZ-positive cells in the lumen of dorsal aorta and those budding from the lining cells of the dorsal aorta (Figure 1D and 1E). Moreover, no blood cells were found within VE-cadherin–deficient embryos, in addition to impaired vascularization.[30] During embryogenesis, vasculogenesis and hematopoiesis are coordinated by hemangioblasts residing in AGM region, including the dorsal aorta.[31] VE-cadherin–expressing cells may function as adult hemangioblasts because VE-cadherin promoter–activated cells were positive for both CD31 and CD45. It should be tested in the future whether GFP-expressing CD45-positive cells in the infarcted area function as cytokine-secreting cells because EPCs are derived from monocytes and secrete angiogenic factors.[2]

It has been controversial whether bone marrow–derived cells are integrated into vasculature.[32,33] By using parabiotic mice model, we demonstrated that cells from extracardiac tissues were incorporated into both pre-existing endothelial cell and VSMC layers (Figure 5C and 5D). Furthermore, we detected VE-cadherin in both vascular layers of infarcted mice (Figure 4G). VE-cadherin promoter-activated cell detected among smooth muscle cells may be either incorporated cell or pre-existing smooth muscle cells. The former cell may use VE-cadherin–dependent cell–cell interaction for incorporation into the smooth muscle layer across the VE-cadherin–expressing endothelial cells on ischemia. Both endothelial cells and VSMCs originate from the same lineage serving as vascular progenitor cells in embryonic stem cells.[34] Even mature vascular endothelial cells can differentiate into smooth muscle cell.[35] It will be necessary to test whether VE-cadherin promoter-activated cells can give rise to the smooth muscle cells to examine the potential function as vascular progenitor cells.

We obtained the data indicative of unidentified factors that drives VE-cadherin promoter in bone marrow and heart. VEGF-induced mobilization of EPCs depends on the expression of Flk-1 expressed on the EPCs as placental growth factor recruits HPCs that express Flt-1.[8,36] It is of note that we find that circulating factors affect the activity of VE-cadherin promoter just in the vessels of the heart, without affecting activity in other organs (supplemental Figure III). By identifying VE-cadherin promoter-activating factors, we may augment neovascularization in combination with EPC-based cell therapy.

In conclusion, VE-cadherin promoter is reactivated in the ischemic tissue vessels and bone marrow–derived cells. Thus, reactivation of VE-cadherin may be involved in the integration of vessel-constituting cells and angiogenic factor–producing cells.

Acknowledgments

This work was supported by grants from the Ministry of Health, Labor, and Welfare of Japan, from the Program for Promotion of Fundamental Studies in Health Sciences of the National Institute of Biomedical Innovation (NIBIO), from the Ministry of Education, Science, Sports and Culture of Japan, and from Takeda Medical Research Foundation. We thank M. Matsuda for comments; S.I. Nishikawa and D. Vestweber for antibodies; P. Huber for VE-cadherin promoter DNA; M. Yanagisawa, and J. Miyazaki for mice; and M. Miyabayashi, and Y. Matsuura for technical assistance.

References

1. Losordo DW, Dimmeler S. Therapeutic angiogenesis and vasculogenesis for ischemic disease: part II: cell-based therapies. *Circulation.* 2004;109:2692–2697.
2. Rehman J, Li J, Orschell CM, March KL. Peripheral blood "endothelial progenitor cells" are derived from monocyte/macrophages and secrete angiogenic growth factors. *Circulation.* 2003;107:1164–1169.
3. Asahara T, Murohara T, Sullivan A, Silver M, van der ZR, Li T, Witzenbichler B, Schatteman G, Isner JM. Isolation of putative progenitor endothelial cells for angiogenesis. *Science.* 1997;275:964–967.
4. Shi Q, Rafii S, Wu MH, Wijelath ES, Yu C, Ishida A, Fujita Y, Kothari S, Mohle R, Sauvage LR, Moore MA, Storb RF, Hammond WP. Evidence for circulating bone marrow-derived endothelial cells. *Blood.* 1998;92:362–367.
5. Urbich C, Dimmeler S. Endothelial progenitor cells: characterization and role in vascular biology. *Circ Res.* 2004;95:343–353.
6. Rafii S, Lyden D. Therapeutic stem and progenitor cell transplantation for organ vascularization and regeneration. *Nat Med.* 2003;9:702–712.
7. Carmeliet P. Mechanisms of angiogenesis and arteriogenesis. *Nat Med.* 2000;6:389–395.
8. Hattori K, Heissig B, Wu Y, Dias S, Tejada R, Ferris B, Hicklin DJ, Zhu Z, Bohlen P, Witte L, Hendrikx J, Hackett NR, Crystal RG, Moore MA, Werb Z, Lyden D, Rafii S. Placental growth factor reconstitutes hematopoiesis by recruiting VEGFR1(+) stem cells from bone-marrow microenvironment. *Nat Med.* 2002;8:841–849.
9. Takahashi T, Kalka C, Masuda H, Chen D, Silver M, Kearney M, Magner M, Isner JM, Asahara T. Ischemia- and cytokine-induced mobilization of bone marrow-derived endothelial progenitor cells for neovascularization. *Nat Med.* 1999;5:434–438.
10. Carmeliet P. Angiogenesis in health and disease. *Nat Med.* 2003;9:653–660.
11. Dejana E. Endothelial cell-cell junctions: happy together. *Nat Rev Mol Cell Biol.* 2004;5:261–270.
12. Navarro P, Ruco L, Dejana E. Differential localization of VE- and N-cadherins in human endothelial cells: VE-cadherin competes with N-cadherin for junctional localization. *J Cell Biol.* 1998;140:1475–1484.
13. Corada M, Mariotti M, Thurston G, Smith K, Kunkel R, Brockhaus M, Lampugnani MG, Martin-Padura I, Stoppacciaro A, Ruco L, McDonald DM, Ward PA, Dejana E. Vascular endothelial-cadherin is an important determinant of microvascular integrity in vivo. *Proc Natl Acad Sci U S A.* 1999;96:9815–9820.
14. Liao F, Li Y, O'Connor W, Zanetta L, Bassi R, Santiago A, Overholser J, Hooper A, Mignatti P, Dejana E, Hicklin DJ, Bohlen P. Monoclonal antibody to vascular endothelial-cadherin is a potent inhibitor of angiogenesis, tumor growth, and metastasis. *Cancer Res.* 2000;60:6805–6810.
15. Weis S, Shintani S, Weber A, Kirchmair R, Wood M, Cravens A, McSharry H, Iwakura A, Yoon YS, Himes N, Burstein D, Doukas J, Soll R, Losordo D, Cheresh D. Src blockade stabilizes a Flk/cadherin complex, reducing edema and tissue injury following myocardial infarction. *J Clin Invest.* 2004;113:885–894.
16. Kawamoto S, Niwa H, Tashiro F, Sano S, Kondoh G, Takeda J, Tabayashi K, Miyazaki J. A novel reporter mouse strain that expresses enhanced green fluorescent protein upon Cre-mediated recombination. *FEBS Lett.* 2000;470:263–268.

17. de Bruijn MF, Ma X, Robin C, Ottersbach K, Sanchez MJ, Dzierzak E. Hematopoietic stem cells localize to the endothelial cell layer in the midgestation mouse aorta. *Immunity*. 2002;16:673–683.
18. Tavian M, Coulombel L, Luton D, Clemente HS, Dieterlen-Lievre F, Peault B. Aorta-associated CD34+ hematopoietic cells in the early human embryo. *Blood*. 1996;87:67–72.
19. Loughna S, Sato TN. Angiopoietin and Tie signaling pathways in vascular development. *Matrix Biol*. 2001;20:319–325.
20. Wright DE, Wagers AJ, Gulati AP, Johnson FL, Weissman IL. Physiological migration of hematopoietic stem and progenitor cells. *Science*. 2001;294:1933–1936.
21. Abkowitz JL, Robinson AE, Kale S, Long MW, Chen J. Mobilization of hematopoietic stem cells during homeostasis and after cytokine exposure. *Blood*. 2003;102:1249–1253.
22. Ismail JA, Poppa V, Kemper LE, Scatena M, Giachelli CM, Coffin JD, Murry CE. Immunohistologic labeling of murine endothelium. *Cardiovasc Pathol*. 2003;12:82–90.
23. Allport JR, Muller WA, Luscinskas FW. Monocytes induce reversible focal changes in vascular endothelial cadherin complex during transendothelial migration under flow. *J Cell Biol*. 2000;148:203–216.
24. Su WH, Chen HI, Jen CJ. Differential movements of VE-cadherin and PECAM-1 during transmigration of polymorphonuclear leukocytes through human umbilical vein endothelium. *Blood*. 2002;100:3597–3603.
25. van Buul JD, Voermans C, van der Berg V, Anthony EC, Mul FP, van Wetering S, van der Schoot CE, Hordijk PL. Migration of human hematopoietic progenitor cells across bone marrow endothelium is regulated by vascular endothelial cadherin. *J Immunol*. 2002;168:588–596.
26. Arai F, Hirao A, Ohmura M, Sato H, Matsuoka S, Takubo K, Ito K, Koh GY, Suda T. Tie2/angiopoietin-1 signaling regulates hematopoietic stem cell quiescence in the bone marrow niche. *Cell*. 2004;118:149–161.
27. Nishikawa SI, Nishikawa S, Hirashima M, Matsuyoshi N, Kodama H. Progressive lineage analysis by cell sorting and culture identifies FLK1+VE-cadherin+ cells at a diverging point of endothelial and hemopoietic lineages. *Development*. 1998;125:1747–1757.
28. Wang L, Li L, Shojaei F, Levac K, Cerdan C, Menendez P, Martin T, Rouleau A, Bhatia M. Endothelial and hematopoietic cell fate of human embryonic stem cells originates from primitive endothelium with hemangioblastic properties. *Immunity*. 2004;21:31–41.
29. Taoudi S, Morrison AM, Inoue H, Gribi R, Ure J, Medvinsky A. Progressive divergence of definitive haematopoietic stem cells from the endothelial compartment does not depend on contact with the fetal liver. *Development*. 2005;132:4179–4191.
30. Gory-Faure S, Prandini MH, Pointu H, Roullot V, Pignot-Paintrand I, Vernet M, Huber P. Role of vascular endothelial-cadherin in vascular morphogenesis. *Development*. 1999;126:2093–2102.
31. Kubo H, Alitalo K. The bloody fate of endothelial stem cells. *Genes Dev*. 2003;17:322–329.
32. Ziegelhoeffer T, Fernandez B, Kostin S, Heil M, Voswinckel R, Helisch A, Schaper W. Bone marrow-derived cells do not incorporate into the adult growing vasculature. *Circ Res*. 2004;94:230–238.
33. Sata M, Saiura A, Kunisato A, Tojo A, Okada S, Tokuhisa T, Hirai H, Makuuchi M, Hirata Y, Nagai R. Hematopoietic stem cells differentiate into vascular cells that participate in the pathogenesis of atherosclerosis. *Nat Med*. 2002;8:403–409.
34. Yamashita J, Itoh H, Hirashima M, Ogawa M, Nishikawa S, Yurugi T, Naito M, Nakao K, Nishikawa S. Flk1-positive cells derived from embryonic stem cells serve as vascular progenitors. *Nature*. 2000;408:92–96.
35. Frid MG, Kale VA, Stenmark KR. Mature vascular endothelium can give rise to smooth muscle cells via endothelial-mesenchymal transdifferentiation: in vitro analysis. *Circ Res*. 2002;90:1189–1196.
36. Hattori K, Dias S, Heissig B, Hackett NR, Lyden D, Tateno M, Hicklin DJ, Zhu Z, Witte L, Crystal RG, Moore MA, Rafii S. Vascular endothelial growth factor and angiopoietin-1 stimulate postnatal hematopoiesis by recruitment of vasculogenic and hematopoietic stem cells. *J Exp Med*. 2001;193:1005–1014.

2007年（平成19年）1月24日（水曜日）

日経産業新聞

子宮内膜から筋肉細胞

筋ジストロフィー治療に道

国立成育医療センター 月経血を利用

国立成育医療センター研究所の梅沢明弘・生殖医療研究部長らのグループは、細胞治療技術を使い、筋ジストロフィーの治療につながる基礎実験に成功した。女性の子宮内膜の細胞から筋肉細胞を作り、欠損するとこの病気になるたんぱく質をマウスの中で作り出した。患者への負担や倫理的な課題のない治療技術につながるとみている。

研究グループはまず、女性ボランティアに提供してもらった月経血を培養した。この血液中には子宮内膜の組織が混ざり、分化の機能を備えた間質細胞も含まれる。この中から約一二%の比率で骨格筋の細胞を分化、成長させた。

筋ジストロフィーは、遺伝子異常によって筋肉の細胞膜にあるジストロフィンというたんぱく質が作られないために発症する。生まれつきジストロフィンたんぱく質を持たない免疫不全のモデルマウスの筋肉に、培養した筋肉細胞を注射した。すると注射した細胞とマウスにもともとある筋肉細胞が融合し、マウスの筋肉細胞から正常なジストロフィンが分泌されるようになったという。

病気の治療への可能性はこれから探る。効果があれば、女性から提供を受けた月経血をもとに筋肉細胞を作り、筋ジストロフィー患者に注射。ジストロフィンを補って症状を改善する治療法につながる可能性がある。

筋肉細胞は骨髄に含まれる体性幹細胞や、受精卵を材料にした胚（はい）性幹細胞（ES細胞）からも作製できる。しかし、骨髄から採取する際に患者への負担が重く、ES細胞利用は倫理面などで課題も多い。月経血を利用する今回の手法は、こうした課題を解決する再生医療として役立つと考えている。

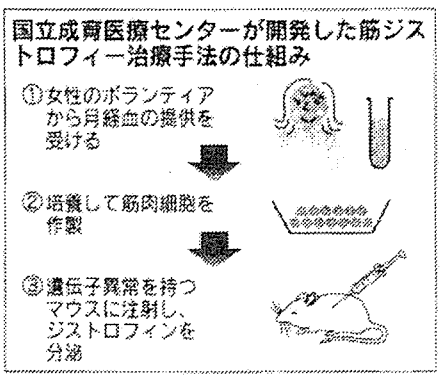

▼筋ジストロフィー　筋肉細胞が徐々に壊れて脂肪細胞に置き換わり、筋肉の機能が失われる難病。進行性で、子供のころに症状が表れ、二十歳代になると呼吸や心臓の機能にも異常が出て死に至ることが多い。原因遺伝子の違いにより様々なタイプに分かれる。最も重いデュシェンヌ型の場合、男性のみがかかり、発症率は約三千五百人に一人。また確立された治療法はないが、遺伝子治療などの研究が進められている。

サイエンス 学び

ドリー遺産 5

生命倫理 問いかける

「毎月平均3、4個のクローン胚を女性の子宮に戻している。日本でも数人のクローンベビーが誕生した」

2002年12月に「世界で初めてクローン人間を誕生させた」と発表した新興宗教団体「ラエリアン」(本部・スイス)の科学者ブリジット・ボワセリエ博士は、1月下旬、読売新聞の電話インタビューに対し、クローン人間作りを今も続けていると答えた。

ただし、博士はクローン人間誕生の科学的な証拠を一切示していない。

国立成育医療センター研究所の阿久津英憲室長は「クローン技術で子供を作ろうとすると、流産や胎盤の異常が必ず起き、母体も危険にさらされることが動物実験から予見される。クローン人間が生まれる確率はゼロに近い」と否定的だ。

ほかにもイタリアの産婦人科医らがクローン人間作製計画を発表したことがあったが、科学界は「信ぴょう性がない」として、今はほとんど無視している。

クローン人間騒動は下火となったが、ドリーが残した問題はそれだけではない。

再生医療などでクローンを研究する科学者たちにとって、クローン胚の元となる卵子は、のどから手が出るほど欲しい研究材料だ。論文捏造事件のソウル大・黄禹錫(ファンウソク)元教授らのグループは、金銭を支払ったり、女性スタッフに圧力をかけたりして卵子を集めた。

科学技術文明研究所の米本昌平所長は、卵子の需要が新たな南北問題を引き起こしはしないかと心配する。「低所得層の多い国では、売血や強制労働が起きやすいように、卵子を先進国の研究者に売るような事態が起きかねない」

米本所長の懸念も含め、ドリー誕生後、生命倫理をめぐる諸問題が提起され、日本にも影響が及んだ。

1978年に英国で初の体外受精児が誕生したのを契機に、生殖補助医療を規制する法律が整備されていた欧州と異なり、日本には法律がないばかりか米国のように国家レベルで生命倫理に関する検討を行う組織もなかった。

だが、ドリー誕生をきっかけに、97年9月、旧科学技術庁が生命倫理委員会を設置した。クローン人間騒動を後追いする形で、00年にクローン技術規制法が急きょ成立するなど、生命倫理問題をいやおうなく政策課題に引きずり上げた。

元ユネスコ国際生命倫理委員長の位田隆一・京都大教授が言う。「クローン羊誕生後の10年は、生命の始まりの問題がクローズアップされた10年だった」。ドリーの最大の遺産は、私たちの目を再び、生命の誕生の瞬間に向けさせたことかもしれない。

(おわり)

(ワシントン・増満浩志、青田昌史、矢沢寛茂、木下聡、芝田裕一が担当しました)

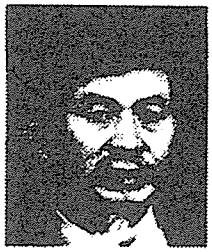

論文捏造を認め、謝罪する黄元教授(AP)

読　売　新　聞

2007年(平成19年) 2月6日 (火曜日)

月経血から筋肉細胞

筋ジストロフィー治療へ注目

女性の月経血に含まれる細胞をマウスに注射し、不足すると筋ジストロフィーを引き起こすたんぱく質を作ることに、国立成育医療センター研究所のグループが成功した。根本的な治療のない筋ジストロフィーの治療につながる成果として注目を集めそうだ。

筋ジストロフィーは、筋肉を動かすジストロフィンと呼ばれるたんぱく質の不足や異常が原因で発病する難病。同研究所生殖医療研究部の梅沢明弘部長らは、女性の月経血に含まれる細胞に着目、ボランティアの女性から提供を受けた月経血を、試験管の中で約3週間培養したところ、筋肉細胞を作ることに成功した。

続いて梅沢部長らは「月経血に含まれる細胞をマウスに注射すれば、体内で筋肉細胞に変化するのでは」と考え、ジストロフィンを先天的に作ることのできないマウスの足に、この細胞を注射した。その結果、約3週間後にマウスの筋肉細胞と注射で移植した細胞が融合し、ジストロフィンを分泌していた。梅沢部長は「月経血に含まれる細胞は子宮内膜細胞と思われ、筋肉細胞に非常になりやすい性質を持っている。できるだけ早く筋ジストロフィーの治療に利用できるように研究を進めたい」と話している。